

Bosons and Fermions near Feshbach resonances

Henning Heiselberg [§]

Univ. of Southern Denmark, Campusvej 55, 5230 Odense M, Denmark

Abstract.

Near Feshbach resonances, $n|a|^3 \gg 1$, systems of Bose and Fermi particles become strongly interacting/dense. In this unitary limit both bosons and fermions have very different properties than in a dilute gas, e.g., the energy per particle approach a value $\hbar^2 n^{2/3}/m$ times an universal many-body constant. Predictions from the LOCV approximation can quantitatively describe recent measurements of trapped Bose and Fermi atoms near Feshbach resonances.

The pairing gap between attractive fermions also scales as $\Delta \sim \hbar^2 n^{2/3}/m$ near Feshbach resonances and is a large fraction of the Fermi energy - promising for observing BCS superfluidity in traps. Pairing undergoes several transitions depending on interaction strength and the number of particles in the trap and can also be compared to pairing in nuclei.

1. Introduction

Recent experiments probe systems of Bosons [1] and Fermions [2, 3, 4, 5] near Feshbach resonances by expansion and RF spectroscopy. The interactions strengths and densities are so large $n^{1/3}|a| \gg 1$ that the dilute gas results no longer apply as, e.g. the energy per particle

$$\frac{E}{N} = 4\pi\hbar^2 \frac{an}{m}, \quad n|a|^3 \ll 1, \quad (1)$$

for bosons and half that for the fermion interaction energy. Instead the strongly or dense limit also known as the unitary limit is encountered where energies (and pairing gaps) are predicted [6, 7] to approach

$$\frac{E}{N} = \text{constant} \times \hbar^2 \frac{n^{2/3}}{m}, \quad n|a|^3 \gg 1, \quad (2)$$

where the universal *constant* is a fundamental many-body parameter that only depends on the spin and the number of spin states of the particle. Several calculations and measurements of this constant now exist as will be discussed in detail below. On dimensional grounds the energy per particle is expected to scale with density as $n^{2/3}$ independent of the scattering length $|a| \rightarrow \infty$. Thus both the Bose and Fermi interaction energies “fermionize” in the unitary limit.

[§] Danish Defense Research Establishment (hh@ddre.dk)

It is implicitly assumed that both the scattering length and the interparticle spacing $r_0 = (3/4\pi n)^{1/3}$ are much larger than the range of interaction which is usually the case for the cold atomic clouds. It is also the case for low density neutron matter since two neutrons are just unbound with 1S_0 scattering length $a = -18$ fm much larger numerically than the typical 1 fm range of nucleon-nucleon interactions. In contrast the neutron and proton are just bound as the deuterium atom.

One of the predictions for the novel scaling laws in the unitary limit for fermions [6] and bosons [7] were based on the lowest order constrained variation (LOCV) approximation. This is a very useful model as it extends from both the dilute to the unitary limit and analytically continues across Feshbach resonances $a \rightarrow \pm\infty$. We shall briefly outline (LOCV) approximation and calculate the energy per particle in detail for both Bose and Fermi atoms in sections 2 and 3 respectively. We will show that the results compares well to recent data on Bosons [1] and Fermions [2, 3, 4] also near Feshbach resonances.

In the remaining sections 4+5 we will discuss BCS pairing in atomic trap with attractive Fermions and draw a connection to pairing in nuclei and nuclear matter.

2. Bosons

The LOCV method was developed for strongly interacting correlated fluids as 4He , 3He and nuclear matter in [8] and has more recently been applied to kaon condensation [9] and strongly interacting fermions [6] and bosons [7]. As explained in these references a good approximation for cold dense systems is the Jastrow wave function $\Psi_J(\mathbf{r}_1, \dots, \mathbf{r}_N) = \prod_{i < j} f(\mathbf{r}_i - \mathbf{r}_j)$ where the pair correlation function $f(r)$ may be determined variationally by minimizing the expectation value of the energy, $E/N = \langle \Psi | H | \Psi \rangle / \langle \Psi | \Psi \rangle$, which may be calculated by Monte Carlo methods that are fairly well approximated by LOCV. The basic idea of this method is that for $r < r_0$ the Jastrow function $f(r)$ approximately obeys the Schrödinger equation for a pair of particles. To take into account many-body effects, which become important when r is comparable to r_0 , the condition is imposed that $f(r > d) = 1$ and $f'(r = d) = 0$ at some healing distance d (e.g., one finds $d = r_0$ in the dilute limit and $d = (2/3)^{1/3}r_0$ in the dense limit). The boundary conditions at short distances is given by the scattering length $(rf)'/rf = -1/a$ at $r = 0$. It is assumed that the range of the two-body interactions is small compared both to $|a|$ and r_0 . Solving the Schrödinger equation gives a wave-function $rf(r) \propto \sin[k(r - b)]$ for positive energy and $rf(r) \propto \sinh[k(r - b)]$ for negative energy. The boundary conditions determine the phase kb , the healing length d as well as the energy. When positive, the energy $E/N = \hbar^2 k^2 / 2m$ can be calculated in terms of the scattering length as (see [7] for details)

$$\frac{a}{d} = \frac{\kappa^{-1} \tan \kappa - 1}{1 + \kappa \tan \kappa}, \quad (3)$$

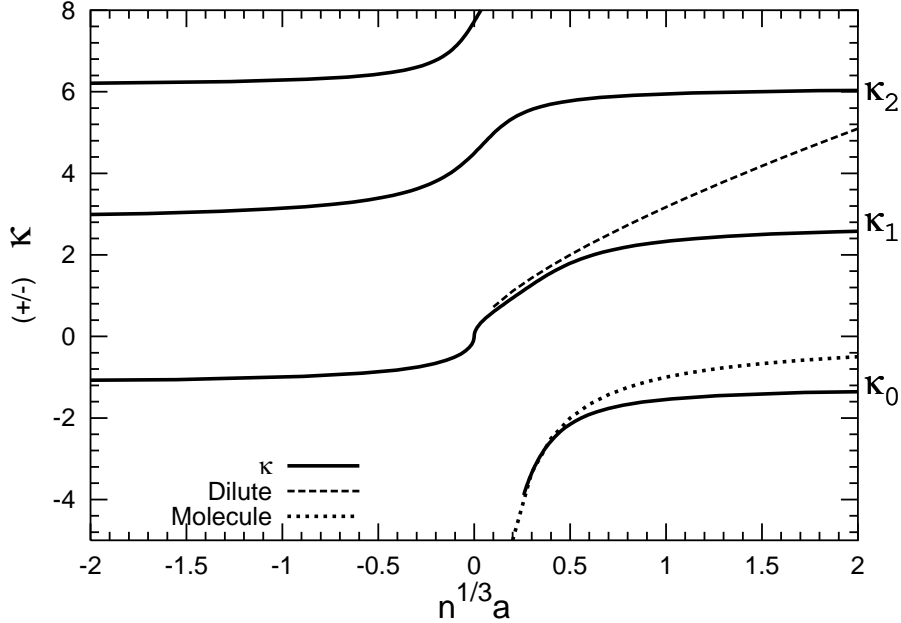


Figure 1. LOCV calculation of the energy per particle in a BEC vs. scattering length. Specifically, $\kappa = kd = \sqrt{|E/N|2md}$ times the sign of the energy is plotted vs. $a/d \simeq an^{1/3}$.

where $\kappa = kd$. The negative energy (dimer) state $E/N = -\hbar^2 k^2/2m$ is determined by

$$\frac{a}{d} = \frac{\kappa^{-1} \tanh \kappa - 1}{1 - \kappa \tan \kappa}. \quad (4)$$

The multiple solutions to these equations corresponding to 0,1,2,3... number of nodes in the (two-body) wave-function $f(r)$ are shown in Fig. (1). As $R \rightarrow 0$ nodes inside the two-body potential and deeply bound states become irrelevant.

In the dilute limit Eqs. (3,4) gives the correct energy per particle Eq. (1). By contrast, when $|a|/r_0$ is large Eq. (3) reduces to $\kappa \tan \kappa = -1$ with solutions $\kappa_1 = 2.798386..$, $\kappa_2 = 6.1212..$, etc., and asymptotically $\kappa_n = n\pi$ for integer n . The negative energy solution (the dimer state) to Eq. (4) reduces to $\kappa \tanh \kappa = 1$ for $a \gg r_0$ with solution $\kappa_0 = 1.1997..$

The energy of a repulsive BEC gas as it approaches a Feshbach resonance, $a \rightarrow +\infty$, is of special interest

$$\frac{E_1}{N} = \left(\frac{3}{2}\right)^{2/3} \frac{\hbar^2 \kappa_1^2}{2mr_0^2} = 13.33\hbar^2 \frac{n^{2/3}}{m}. \quad (5)$$

These energies can be compared to the JILA experiment [1] where the scattering length is tuned near the Feshbach resonance by a magnetic field B as

$$a(B) = a_{bg} \left(1 - \frac{\Delta}{B - B_{Feshbach}}\right). \quad (6)$$

Coherent atom-molecule oscillations are induced in the BEC at a frequency $\nu(B)$. We take this frequency as the difference between the mean field energy of two atoms in the

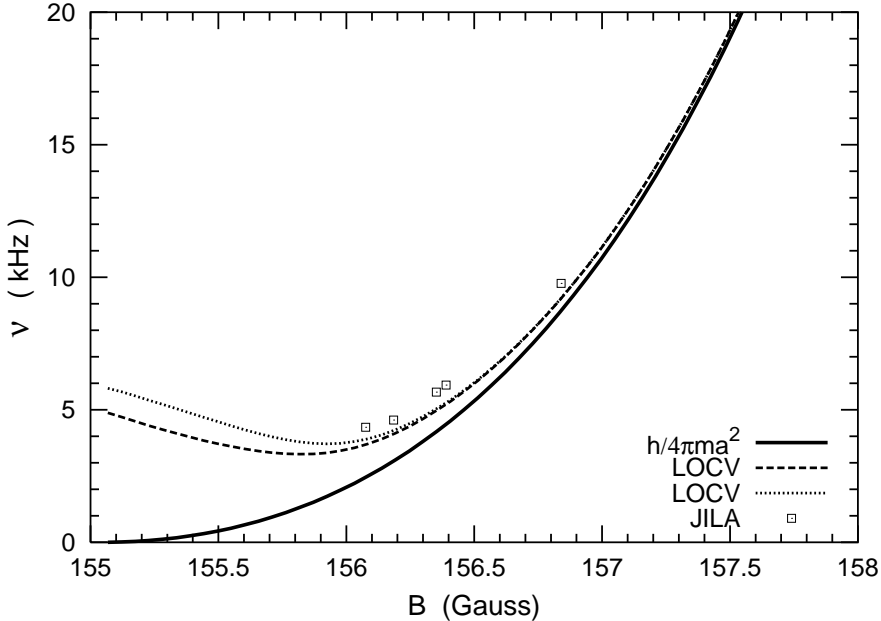


Figure 2. Frequency of the atomic-molecular transition in a ^{85}Rb BEC as function of magnetic field near the Feshbach resonance. The full curve is the in vacuum transition frequency for two atoms to a molecule $\hbar/2\pi ma^2$. The in medium LOCV predictions for a many-body system (see text) are shown with dotted and dashed curves for the transition to a dimer and to a molecule in vacuum respectively. Data from JILA [1].

atomic state and the molecular state

$$\nu = \frac{1}{h} \left(2\frac{E}{N} + \frac{\hbar^2}{ma^2} \right) = \frac{\hbar}{2\pi m} \left(\kappa^2 d^{-2} + a^{-2} \right) \quad (7)$$

which is shown in Fig. (2) where also the energy difference to the dimer state is shown. Off resonance there is little difference whereas close to the resonance they differ by $\hbar^2 \kappa_0^2 / 2\pi m d^2$. Whereas the molecule frequency vanish at the Feshbach resonance the in medium ones approaches a constant value in LOCV which according to Eqs. (7) and (5) is $\nu = \hbar \kappa_1^2 / 2\pi m d^2 = 2.12 \hbar n^{2/3} / m$ for the transition of two atoms in the unitary limit to a molecular state in vacuum. For the ^{85}Rb BEC of average density $n = 2 \times 10^{-12} \text{ cm}^{-3}$ [1] it gives a frequency $\nu = 5.0 \text{ kHz}$ at the Feshbach resonance.

As seen in Fig. (2) the calculated transition frequency is in nice agreement with the JILA data. The calculated frequencies have a minimum just above the resonance of order $\sim 4 \text{ kHz}$ because the atomic energy decrease faster with detuning (i.e., decreasing scattering length) than the molecular energies. The LOCV calculations are more reliable up to $an^{1/3} \lesssim 1$ whereas above, i.e. close to the Feshbach resonance $B \simeq 155 \text{ G}$ higher order corrections may affect the frequency quantitatively.

The absence of experimental data in the 155-156G region is due to overdamping of the atom-molecule oscillations. The imaginary part of the self-energies may be so large near the Feshbach resonance that the quasi-particle are not well defined.

The finite (effective) range of the interaction modifies the scattering length off the

resonance in Fig. (2), and it increases the frequency slightly for $B \gtrsim 157$ G [10] improving the agreement with data.

The depletion of the condensate can also be calculated in the LOCV approximation from $f(r)$. The condensate fraction is [7]

$$\frac{n_0}{n} = 1 - n \int [1 - f(r)]^2 d^3r = \left(\frac{d}{r_0} \right)^3 \left[\frac{6}{\kappa^3} (\sin \kappa - \kappa \cos \kappa) - 1 \right]. \quad (8)$$

which predicts quenching of the BEC for $na^3 \gtrsim 0.6$. The condensate fraction differs from the dilute limit given by $n_0/n = 1 - (4/\sqrt{3}\pi)(a/r_0)^{3/2}$, as well as from hard-sphere potential and exact quantum Monte Carlo calculations.

3. Fermions

In the unitary limit, $n|a|^3 \gg 1$, a system of fermions is dense and/or strongly interacting. The energy per particle has been calculated within Galitskii resummation, the LOCV method and recently by fixed node Green's function Monte Carlo (FN-GFMC). They find that the interaction energy does not extrapolate to $\pm\infty$ as the dilute result of Eq. (1) does, but approaches a universal constant times the kinetic or Fermi energy, $E_F = \hbar^2 k_F^2 / 2m$, as in Eq. (2)

$$\frac{E}{N} = E_{kin} + E_{int} = \frac{3}{5} E_F [1 + \beta]. \quad (9)$$

Here, $\beta = E_{int}/E_{kin}$ is a universal many-body parameter, which only depends on the number of spin states ν_s ($n = \nu_s k_F^3 / 6\pi$). For two spin states β is displayed in Table 1 for the various calculations as will be described in the following subsections. Recent measurements [2, 3, 4] of β seem to confirm this unitary limit near Feshbach resonances.

3.1. Galitskii resummation

The scattering amplitude $f = -a(1 - ika)/(1 + k^2 a^2)$ for particle of momentum $k \sim k_F$ changes from the scattering length to $\sim ik_F^{-1}$ in the unitary limit. Galitskii resummation of ladder diagrams [11] also leads to $\sim k_F^{-1}$ scaling of the real part of the scattering amplitude [6]. Brueckner, Bethe and Goldstone [12] pioneered such studies for nuclear matter and 3He for the more complicated cases, where the range of interactions, scattering lengths and repulsive cores all are comparable in magnitude. In our case the range R of interaction is small, $k_F R \ll 1$, and therefore all particle-hole diagrams are negligible. This is opposite to electro-magnetic interactions where the strength of the interaction is small but the range of interactions is large and must be screened by Debye or Landau damping implicit in loop diagrams. In the Galitskii resummation all higher order particle-particle and hole-hole diagrams are found to contribute to the same order when $k_F a \gg 1$. Due to the very restricted phase space such higher order terms are usually neglected as in standard Brueckner theory. Truncating the resummation to second order one finds for two spin states [6] that $\beta = -175/27(11 - 2 \ln 2) = -0.67$.

Table 1. Calculations and measurements of the ratio of interaction to kinetic energy $\beta = E_{int}/E_{kin}$ in the dense/strongly interacting regime $a \rightarrow -\infty$ for two spin states.

$-\beta$	Calc./Exp.	Reference
0.67	Galitskii approx.	[6]
0.43	LOCV approx.	[6]
0.56	FN-GFMC	[15]
0.26 ± 0.07	Duke exp.	[2]
0.3-0.4	ENS exp.	[3]

The interaction energy is more generally given by the direct minus the exchange interactions and thus proportional to the number of spin states minus one, $\beta(\nu_s) = (\nu_s - 1)\beta(\nu_s = 2)$. This has the remarkable consequence that the energy per particle in the dense and strongly interacting limit is positive for two spin states but negative for four or more spin states. Three spin states seems marginal. Therefore two spin states are stable towards collapse as has recently been confirmed for a ${}^6\text{Li}$ and ${}^{40}\text{K}$ gases near Feshbach resonances. It has long been known that neutron star matter [13] with two spin states likewise has positive energy at all densities whereas for nuclear matter with two spin and two isospin states, i.e. $\nu_s = 4$, the energy per particle is negative and unstable towards collapse and subsequent implosion, spinodal decomposition and fragmentation at subnuclear densities[14]. Above nuclear saturation densities, $k_F R \gtrsim 1$ short range repulsion stabilizes matter up to maximum masses of neutron stars $\sim 2.2M_\odot$.

3.2. LOCV

Information on the energy as function of scattering length and density can be obtained independently from the LOCV approximation. The interaction energy $E_{int} = \kappa^2/2md^2$ calculated above for bosons should be reduced by a factor $(\nu_s - 1)/\nu_s$ due to exchange. If we ignore finite crystal momentum effects and simply add it to the kinetic energy, we obtain

$$\frac{E}{N} = \frac{3}{5}E_F + \frac{\nu_s - 1}{\nu_s} \frac{\kappa^2}{2md^2}. \quad (10)$$

In the case of $\nu_s = 2$ spin states the energy approaches as $a \rightarrow -\infty$

$$\frac{E}{N} = \frac{3}{5}E_F - \frac{\kappa_0^2}{4md^2} = \frac{3}{5}E_F \left[1 - \left(\frac{2}{3\pi} \right)^{2/3} \frac{5}{6} \kappa_0^2 \right], \quad (11)$$

from which we obtain $\beta = -\kappa_0^2(2/3\pi)^{2/3}5/6 = -0.427$.

3.3. Fixed-node Green's function Monte Carlo

In Ref. [15] the energy of a finite number of Fermions in a box has been calculated within FN-GFMC at a Feshbach resonance. Since the gas is in a meta-stable state with

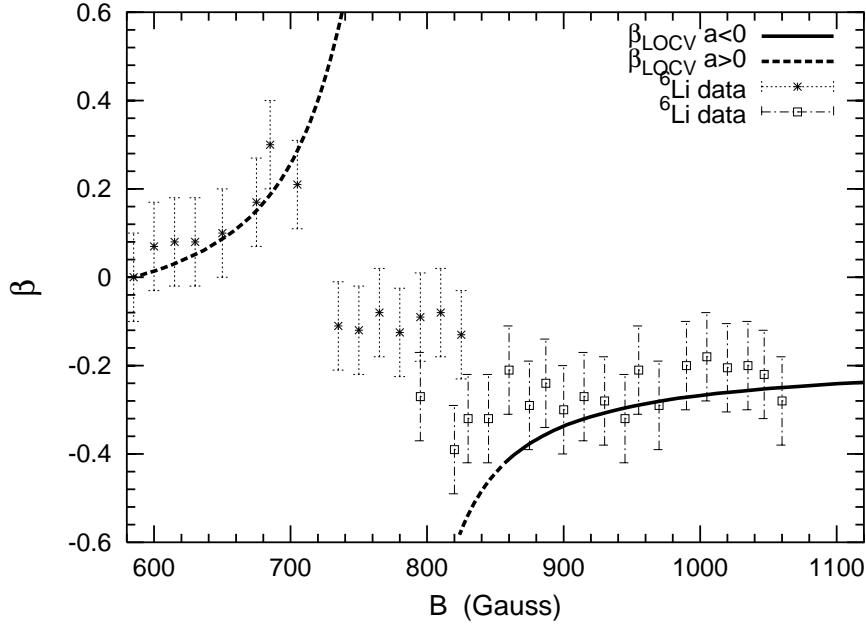


Figure 3. Ratio β of the interaction energy over the kinetic energy vs. magnetic field for ${}^6\text{Li}$. Data is taken from [3]. Predictions from Eq. (10) with κ calculated within LOCV are shown with full and dashed curves for negative and positive scattering length respectively. The density and scattering length vs. magnetic field near the Feshbach resonance at 855G is taken from [3].

typical ~ 40 lower lying molecular states, the number of nodes in the Jastrow or two-body wave-function must be fixed. At the Feshbach resonance $a \rightarrow -\infty$ they find that the energy of the system increase with the number of particles as $E = (1 + \beta)NE_{\text{kin}}$ with $\beta = -0.56 \pm 0.01$.

Pairing favors an even number of particles and from the odd-even staggering of $E(N)$ a pairing gap $\Delta \simeq 0.54E_F$ is extracted from the FN-GFMC calculations at the Feshbach resonance.

3.4. Experiments

Several experiments with trapped Fermi atoms have recently measured energies in the strongly interacting or dense limit near Feshbach resonances. Trivial correction factors [2] relate the finite trap results to the bulk limit results discussed above.

The Duke group [2] measured the energy of ${}^6\text{Li}$ Fermi atoms near a Feshbach resonance from expansion energies. After correcting for thermal energies, they find $\beta = -0.27 \pm 0.01$.

Bourdell et al. at ENS [3] measure expansion energies for ${}^6\text{Li}$ near a Feshbach resonance. They find $\beta = -0.4 \pm 0.1$ as $a \rightarrow -\infty$ as shown in Fig. (3). The situation is more complicated at the other side of the resonance, $a \rightarrow +\infty$, where the ratio increases up to $\beta = 0.2 \pm 0.1$ in agreement with LOCV predictions, but then drops to a plateau

close to the resonance. Formation of molecules in the plateau region is speculated to be responsible for the plateau. A somewhat similar behavior was found in the MIT experiment [5] that measures the transition frequency between three hyperspin states of ^6Li , whereas a similar experiment at JILA on ^{40}K [4] does not find a such plateau. The experiments do, however, confirm the unitary limitation to energies and frequencies.

The LOCV calculations compare well to data as $a \rightarrow -\infty$ whereas $\beta(a \rightarrow +\infty)$ exceeds the data especially at the plateau. Whether this is due to molecule formation or finite temperature, which can have a strong effect on β [16], should be investigated.

4. Pairing of fermi atoms in harmonic oscillator traps

BCS pairing and superfluidity is expected for trapped Fermi atoms with attractive interactions. As atomic gases have widely tunable number of particles, densities, interaction strengths, temperatures, spin states, and other parameters, they hold great promise for a more general understanding of pairing phenomena in solids, metallic clusters, grains, nuclei, neutron stars and quark matter.

In a uniform dilute gas with sufficiently strong interactions or large number of particles the bulk limit is reached, and the pairing gap is at zero temperature [17, 18]

$$\Delta = E_F \frac{8}{e^2} (4e)^{\nu_s/3-1} \exp \left[\frac{\pi}{2ak_F} \right]. \quad (12)$$

In the unitary limit, $k_F|a| \gtrsim 1$, the pairing gap approaches a finite fraction of the Fermi energy [6] just as the energy per particle. The FN-GFMC calculations discussed above [15] find that the odd-even staggering energy or pairing gap in bulk is $\Delta \simeq 0.54E_F$ which is quite close the value $\Delta \simeq 0.49E_F$ obtained by extrapolating Eq. (12) to $a \rightarrow -\infty$ for two spin states.

Near a Feshbach resonance the strongly interacting Fermi gas becomes unstable towards molecule formation and the critical temperature $T_c = (\gamma/\pi)\Delta \simeq 0.567\Delta$ for BCS superfluidity is expected to cross-over towards the slightly smaller critical temperature for forming a Bose-Einstein condensate of molecules [19, 20]. If we take $\Delta = 0.54E_F$ from FN-GFMC both the BCS and BEC critical temperatures, $T_c \simeq 0.5\Delta$, are therefore around or above the lowest temperatures reported for trapped Fermi atoms [5, 2, 3, 4]. This bodes well for observing BCS superfluidity in atomic traps and establishing the unitary scaling of pairing gaps.

As cooling improves further and smaller pairing gaps may be found, new pairing regimes take over that are important in other systems as solids, nuclei, neutron stars, etc. We shall outline the various pairing regimes shown in Fig. (4) vs. density interaction strength and relate it to BCS pairing in bulk.

The various pairing regimes shown in Fig. (4) can, except from the dense or unitary limit, be calculated from in the dilute limit Hamiltonian

$$H = \sum_{i=1}^N \left(\frac{\mathbf{p}_i^2}{2m} + \frac{1}{2}m\omega^2\mathbf{r}_i^2 \right) + 4\pi\hbar^2 \frac{a}{m} \sum_{i < j} \delta^3(\mathbf{r}_i - \mathbf{r}_j), \quad (13)$$

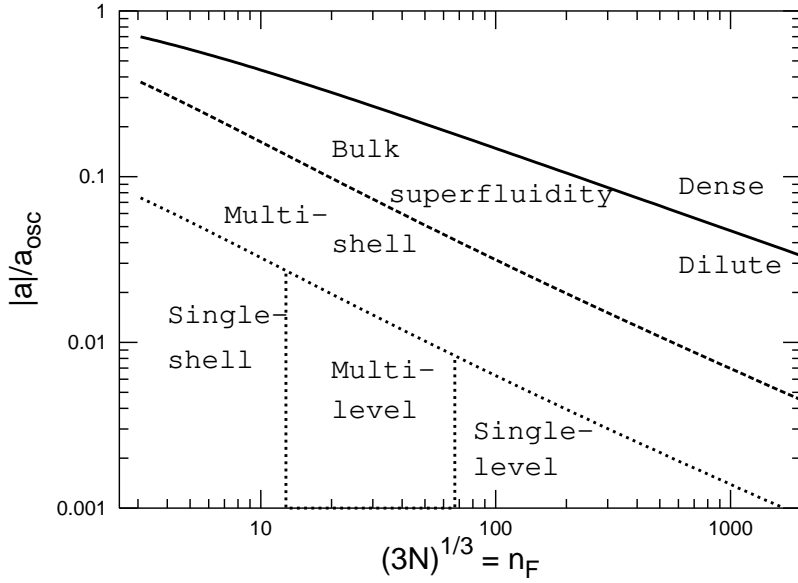


Figure 4. Diagram displaying the regimes for the various pairing mechanisms (see text) at zero temperature in h.o. traps vs. the number of particles $N = n_F^3/3$ and the interaction strength $a < 0$. The dotted lines indicate the transitions between single-shell pairing $\Delta = G$, multi-level, single-level, and multi-shell pairing. At the dashed line determined by $2G \ln(\gamma n_F) = \hbar\omega$ the pairing gap is $\Delta \simeq \hbar\omega$, and it marks the transition from multi-shell pairing to bulk superfluidity Eq. (12). The pairing gap is $\Delta = 0.54E_F$ above the full line $n|a|^3 \geq 1$, which separates the dilute from the dense gas. From [23]

for N atoms in a spherical harmonic oscillator (h.o.) potential. When energies are measured in units of $\hbar\omega$, and lengths in $a_{osc} = \sqrt{\hbar/m\omega}$ only two parameters remain in the Hamiltonian, namely the number of particles and the interaction strength as plotted in Fig. (4)

When the traps contain relatively few atoms that are weakly interacting (lower left corner of Fig. (4)) the level spectra are highly degenerate due to the SU(3) symmetry of the spherical h.o. potential. Due to the Pauli principle the h.o. shells $n = 0, 1, \dots, n_F$ are filled up. Only the top Fermi shell $n_F \simeq (3N)^{1/3}$, where N is the number of Fermi atoms, may be partially filled. The levels with angular momentum $l = n_F, n_F - 2, \dots, 1$ or 0 are all degenerate in the weakly interacting limit due to SU(3) symmetry. This enhances pairing as the gap generally increases with the number of states and leads to a supergap [21]

$$G = \frac{32\sqrt{2n_F}}{15\pi^2} \frac{|a|}{a_{osc}} \hbar\omega. \quad (14)$$

For stronger interactions multi-shell pairing also takes place whereas for more particles the stronger mean field causes level splitting, which reduces pairing towards single level pairing [21, 22, 23] and shows up as a distinct shell structure with h.o. magic numbers.

Varying the number of particles and interaction strengths thus allows us to investigate a wide range of pairing mechanisms that apply to many other physical

systems, e.g., nuclei and neutron stars as will be discussed in the following section.

5. Pairing in nuclei and nuclear matter

The nuclear mean field is often approximated by a simple h.o. form and the residual effective pairing interaction by a delta force in order to obtain some qualitative insight into single particle levels, pairing, collective motion, etc., (see, e.g., [24, 25]). We can therefore compare pairing in nuclei to that in traps as investigated above, once the h.o. potential is adjusted to describe nuclei.

As described in [23] the anharmonic nuclear mean field is stronger and of opposite sign than that in atomic traps. It also contains a strong spin-orbit force which change the magic numbers from the h.o. shells. Correcting for that the quasi-particle energies and pairing gaps were calculated by solving the Bogoliubov-deGennes equations which can be expressed as gap equation. The pairing depends only on one parameter, namely the effective scattering length in the Hamiltonian $a = -0.41\text{fm}$ that was obtained from fitting the pairing gaps to the odd-even staggering binding energies of neutrons and protons in nuclei (see Fig. 5). The shell structure and the average pairing is well reproduced. If nuclei were to be placed in the pairing phase diagram of Fig. (4) they would lie in the transition region between the single-shell, multi-shell and single-level pairing regions. Because the multi-shell increase pairing and single-level decrease pairing the average gaps are to a good approximation given by the supergap of Eq. (14). Adjusting the h.o. frequency and oscillator length to that in nuclei with constant central densities of $n = 0.15\text{fm}^{-3}$ the supergap becomes

$$\Delta \simeq G = \frac{|a|}{0.41\text{fm}} \frac{5.5\text{MeV}}{A^{1/3}}. \quad (15)$$

The supergap predicts a $A^{-1/3}$ scaling in good agreement with nuclear pairing data. It differs slightly from the standard $A^{-1/2}$ scaling in the Bethe-Weiszäcker liquid-drop formula.

The supergap is robust in the sense that it does not depend on the level spectra or other details, and thus allows us to extract the effective scattering length directly.

For very large nuclei multi-shell pairing becomes increasingly important and pairing approaches that in bulk matter. With the effective nucleon coupling constant $a = -0.41\text{fm}$ extracted from pairing gaps in finite nuclei, we can estimate the 1S_0 pairing of both neutrons and protons in nuclear matter from Eq. (12)

$$\Delta \simeq 1.1\text{MeV}. \quad (16)$$

Neutron star matter has a wide range of densities and is very asymmetric, $Z/A \simeq 0.1$. One can attempt to estimate of the pairing gaps as function of density from the gap in bulk, Eq. (12), with $a \simeq -0.41\text{ fm}$. However, the effective interaction a is density dependent. At higher densities we expect the effective interaction to become repulsive as is the case for the nuclear mean field at a few times nuclear saturation density. At lower densities the effective scattering length should approach that in vacuum which for neutron-neutron scattering is $a(^1S_0) \simeq -18\text{ fm}$.

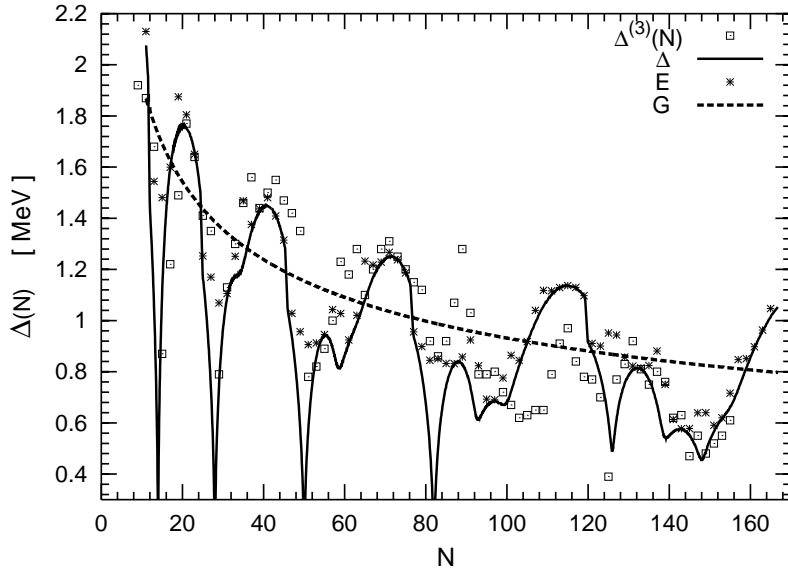


Figure 5. Neutron pairing $\Delta^{(3)}(N)$ vs. the number of neutrons. The experimental values have been averaged over isotopes [26]. The calculated gaps Δ and quasi-particle energies E are obtained from the gap equation (see text) with effective coupling strength $a = -0.41$ fm. The supergap G is shown with dashed line. From [23].

Neutron stars are so cold that neutron and proton superfluidity is expected in most of the surface layers. The depinning of superfluid vortices can explain neutron star glitches in star quakes [28].

6. Summary and Outlook

We list the main results discussed above and add a few topics for future investigation:

- In the unitary limit near Feshbach resonances, $n|a|^3 \gg 1$, where bosons and fermions interact strongly or are dense, the particle energies (and pairing gaps) scale like $\hbar^2 n^{2/3}/m$ times an universal constant.
- For ^{85}Rb bosons recent experiments [1] confirm the unitary limit and measure a transition frequency $\nu \simeq 4\text{kHz}$ near the Feshbach resonance in agreement with the predictions from LOCV. Experiments at other densities are underway to check the “fermion” $n^{2/3}$ dependence of the energy per particle.
- The unitary limit has also been confirmed for Fermi atoms near Feshbach resonances. Measurements of the universal parameter $\beta = E_{int}/E_{kin} \simeq -0.5$ as $a \rightarrow -\infty$ are compatible with theoretical predictions.
- The pairing gap in traps with attracting Fermi atoms is $\Delta \simeq 0.5E_F$ near Feshbach resonances and the critical temperature $T_c \simeq 0.5\Delta$. Thus superfluidity may already have been achieved in recent experiments.

- Cooling further will eventually make measurements of smaller pairing gaps possible. By varying the number of particles and interaction strengths the pairing in h.o. traps with dilute or dense attractive Fermi atoms undergoes several pairing phases in which a wide range of pairing mechanisms takes place that apply to many other physical systems.
- Pairing of neutrons and protons in nuclei is similar to super-pairing in atomic traps. The supergap scales as $\Delta \simeq 5.5 \text{ MeV}/A^{1/3}$ with mass number. Nuclei also extend into the multi-level pairing regime seen as a strong shell dependence with magic numbers.
- Large nuclei approach the 1S_0 pairing bulk in nuclear matter $\Delta \simeq 1.1 \text{ MeV}$ for both neutrons and protons. Pairing will, however, vary with density and asymmetry in neutron star matter. Low neutron densities is also dominated by a large negative scattering length $a(^1S_0) \simeq -18 \text{ fm}$ due to a Feshbach resonance in the NN channel.
- Mixing fermionic with bosonic atoms allow sympathetic cooling [27, 5] and thus to study weaker pairing. Induced interactions between fermions and bosons generally enhance pairing [18].
- A systems of fermions with attractive interactions and two spin states will not collapse as bosanovae and supernovae, not even near a Feshbach resonance because the kinetic energy dominates, $\beta \geq -1$. If three or more spin states can be tuned resonantly, however, their attractive interaction energy should dominate as $a \rightarrow -\infty$ and the systems collapse as Ferminovae.
- Optical lattices in current experiments have few atoms in each local trap and we thus expect superpairing which favors the insulator vs. conductor state.

Tabletop experiments at low temperatures allow us to study strongly interacting and dense Fermi and Bose systems with unitary scaling, and may provide new insight into BCS pairing in atomic traps. At certain interaction strengths and particle number these are similar to pairing and superfluidity in nuclei and neutron star matter.

References

- [1] N. Claussen et al., Phys. Rev. **A 67**, 060701 (2003).
- [2] K. M. O'Hara, S. L. Hemmer, M. E. Gehm, S. R. Granade, J. E. Thomas, Science Dec 13 2002: 2179-2182. M. E. Gehm, S. L. Hemmer, S. R. Granade, K. M. O'Hara, J. E. Thomas, cond-mat/0212499.
- [3] T. Bourdel et al., cond-mat/0303079.
- [4] C. A. Regal, D. S. Jin, cond-mat/0302246; cond-mat/0305028.
- [5] S. Gupta et al., Science, Vol. 300 (2003), 1723; cond-mat/0306050; cond-mat/0307088.
- [6] H. Heiselberg, Phys. Rev. **A 63**, 043606 (2001); Recent Progress in Many-Body Theories (MBX 1999) (cond-mat/0002056).
- [7] S. Cowell, H. Heiselberg, I.E. Mazets, J. Morales, V.R. Pandharipande, and C.J.Pethick, Phys. Rev. Lett. **88** (2002) 210403
- [8] V. R. Pandharipande, Nucl. Phys. A **174**, 641 (1971) and **178**, 123 (1971); V.R. Pandharipande and H.A. Bethe, Phys. Rev. C **7**, 1312 (1973); V. R. Pandharipande and K. E. Schmidt, Phys. Rev. A **15**, 2486 (1977).
- [9] J. Carlson, H. Heiselberg, and V. R. Pandharipande, Phys. Rev. C **63**, 017603 (2001).
- [10] H.A. Duine and H.T.C. Stoof, cond-mat/0303230, to appear in New J. Physics Focus Issue on Quantum Gases.
- [11] V. M. Galitskii, JETP **34**, 151 (1958).
- [12] K.A. Brueckner, C.A. Levinson, and H.M. Mahmoud, Phys. Rev. **103**, 1353 (1956); H.A. Bethe and J. Goldstone, Proc. Roy. Soc. (London), **A238**, 551 (1957).
- [13] V. R. Pandharipande, Int. J. of Mod. Phys. **B13**, 543 (1999); G. Baym and C. J. Pethick, Ann. Rev. Astr. & Astrophysics **17**, 415 (1979). H. Heiselberg and V.R. Pandharipande, Ann. Rev. Nucl. & Part. Science **50** (2000) 481. H. Heiselberg and M. Hjorth-Jensen, Phys. Rep. **50** (2000) 481.
- [14] H. Heiselberg, C.J.Pethick, D.G.Ravenhall, Phys. Rev. Letts. **61**, 818 (1988).
- [15] J. Carlson, S-Y. Chang, V. R. Pandharipande, K. E. Schmidt, Phys. Rev. Letts. **91**, 50401 (2003).
- [16] T-L. Ho, E. J. Mueller, cond-mat/0306187.
- [17] L. P. Gorkov & T. K. Melik-Barkhudarov, JETP **13**, 1018 (1961);
- [18] H. Heiselberg, C. J. Pethick, H. Smith and L. Viverit, Phys. Rev. Letts. **85**, 2418 (2000).
- [19] P. Nozières and S. Schmidt-Rink, J. Low Temp. Phys. **59**, 195 (1982). C. A. R. Sá de Melo, M. Randeria, and J. R. Engelbrecht, Phys. Rev. Lett. **71**, 3202 (1993).
- [20] H. T. C. Stoof, M. Houbiers, C. A. Sackett, and R. G. Hulet, Phys. Rev. Lett. **76**, 10 (1996).
- [21] H. Heiselberg and B. R. Mottelson, Phys. Rev. Lett **88**, 190401 (2002).
- [22] G. M. Bruun and H. Heiselberg, Phys. Rev. A **65**, 053407 (2002).
- [23] H. Heiselberg, physics/0304005.
- [24] A. Bohr and B. R. Mottelson, *Nuclear Structure* Vols. I+II, Benjamin, New York 1969.
- [25] A. L. Fetter and J. D. Walecka, *Quantum Theory of Many-Particle Systems*, McGraw-Hill 1971.
- [26] G. Audi and A. H. Wapstra, Nucl. Phys. **A595**, 409 (1995). J. Dobaczewski et al., Phys. Rev. **C63**, 024308 (2001).
- [27] H. T. C. Stoof, Phys. Rev. **A61**, 053601 (1999).
- [28] A. Bohr, B. R. Mottelson, D. Pines, Phys. Rev. **110**, 936 (1958).